EPI International Journal of Engineering
Volume 8, Number 1, February 2025, pp. 34-44
DOI: 10.25042/epi-ije.022025.06

*p*ISSN 2615-5109
*e*ISSN 2621-0541

Design of Quasi-isotropic Rectangular Plates for Optimizing the Fundamental Mode of Bending Vibration

Yoshihiro Narita[a,*]

[a]Hokkaido University (Professor Emeritus), Sapporo, Japan. Email: ynarita1951@gmail.com

Abstract

This study is the first work to demonstrate that quasi-isotropic laminated composite plates can be optimized for bending vibration through appropriate stacking sequence design. A quasi-isotropic plate is defined as a laminated composite plate exhibiting isotropic in-plane stiffness. Owing to this constraint, such plates have traditionally been excluded from stacking sequence optimization. The present work clarifies why optimization remains feasible despite the in-plane isotropy requirement and outlines a systematic procedure for maximizing or minimizing the fundamental natural frequency with respect to ply orientation angles while preserving isotropic in-plane behavior. Numerical results are provided for square and rectangular plates under various classical boundary conditions, and the corresponding maximum and minimum fundamental frequencies are identified. In particular, the ratio of maximum to minimum fundamental frequency is evaluated; for example, it reaches 2.17 for a cantilevered quasi-isotropic square plate.

Keywords: Free vibration; rectangular plate; quasi-isotropy; stacking sequence optimization; fundamental frequency

1. Introduction

Laminated composite plates are widely used as structural components in aeronautical and other advanced engineering applications [1–3]. Their high specific strength and stiffness allow significant weight reduction, and they provide considerable potential for structural optimization through stacking-sequence tailoring [4–6]. In vibration design, the stacking sequence can be adjusted to control dynamic behavior; for example, the fundamental natural frequency may be maximized to prevent resonance [7–12].

In contrast, a certain type of laminated plates is designed to suppress anisotropy by adopting specific stacking sequences, since structural plate elements may be subjected to in-plane loads acting in uncertain directions. Such laminates are referred to quasi-isotropic plates, and they have been investigated from various perspectives. Fukunaga [13] studied a class of laminated composites that present isotropic stiffness with respect to both in-plane and out-of-plane stiffnesses. Paradies [14] proposed a method for laminated composites with quasi-isotropic stiffness, and derived the diagram of quasi-isotropic laminates. Akkerman [15] derived the three-dimensional thermoelastic properties of quasi-isotropic laminates in closed form equations. Douglas et al. [16] studied the experimental determination of the elastic modulus of a quasi-isotropic laminate by tensile mechanical testing. Vannucci and Verchery [17] proposed new kinds of isotropic laminates composed of identical anisotropic layers to obtain fully isotropy. Altunsaray and Bayer [18] studies the maximum deflection and free vibration of quasi-isotropic clamped or supported rectangular plates.

By the present definition, a quasi-isotropic laminate is designed to exhibit identical in-plane stiffness in all directions; that is, its in-plane stiffness remains the same regardless of the loading direction within the laminate plane. This character is achieved by orienting individual layers at different angles—for example, 0°, 45°, 90°, and −45° relative to a reference direction, as illustrated in Fig. 1. Nevertheless, the out-of-plane (bending) stiffness of the laminate remains anisotropic. In other words, although the laminate behaves isotropically under in-plane loading, it still exhibits directional dependence in bending vibration.

The present study considers quasi-isotropic plates as candidates for stacking-sequence optimization for the first time. Numerical investigations demonstrate that the fundamental bending frequency can be designed through appropriate stacking sequence under quasi-isotropic constraints. These results confirm that layer-sequence optimization is both effective and feasible for quasi-isotropic rectangular plates.

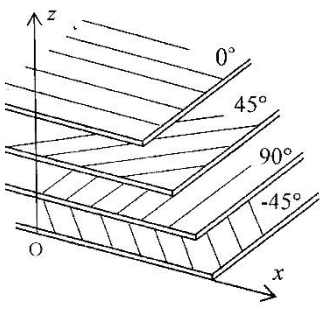

Figure 1. Example of upper half stacking design in a quasi-isotropic symmetric 8-layer laminated plate [0°/45°/90°/-45°]s

*Corresponding author.
Hokkaido University, N-13, W-8, Sapporo
Japan

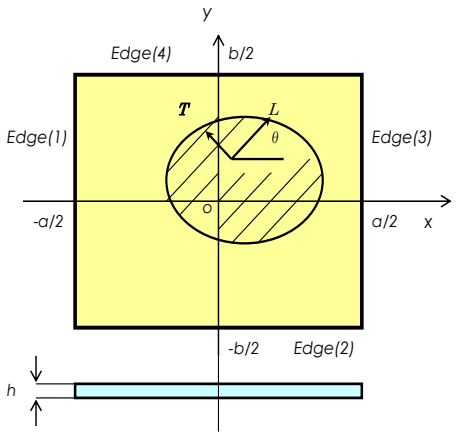

Figure 2. Rectangular plate in the coordinate system

2. Theory

2.1 Quasi-isotropic plate

The present paper deals with quasi-isotropic plates that fall into a class of symmetrically laminated plates with specific stiffness property. In each layer, the stress-strain relation is given in the *k*-th layer [1,2] by

$$\begin{Bmatrix}\sigma_x\\ \sigma_y\\ \tau_{xy}\end{Bmatrix}^{(k)} = \begin{bmatrix}\bar{Q}_{11} & \bar{Q}_{12} & \bar{Q}_{16}\\ \bar{Q}_{12} & \bar{Q}_{22} & \bar{Q}_{26}\\ \bar{Q}_{16} & \bar{Q}_{26} & \bar{Q}_{66}\end{bmatrix}^{(k)} \begin{Bmatrix}\varepsilon_x\\ \varepsilon_y\\ \gamma_{xy}\end{Bmatrix} \tag{1}$$

where σ_x, σ_y and τ_{xy} are normal and shear stresses, and $\varepsilon_x, \varepsilon_y$ and γ_{xy} are normal and shear strains, respectively. $\bar{Q}_{ij}^{(k)}$ (i, j=1,2,6) are the material constants obtained by

$$\begin{aligned}
Q_{11}^{(k)} &= Q_{11}l^4 + 2\left(Q_{12}+2Q_{66}\right)l^2m^2 + Q_{22}m^4\\
\bar{Q}_{12}^{(k)} &= Q_{12}\left(l^4+m^4\right) + \left(Q_{11}+Q_{22}-4Q_{66}\right)l^2m^2\\
\bar{Q}_{22}^{(k)} &= Q_{11}m^4 + 2\left(Q_{12}+2Q_{66}\right)l^2m^2 + Q_{22}l^4\\
\bar{Q}_{16}^{(k)} &= \left(Q_{11}-Q_{12}-2Q_{66}\right)l^3m - \left(Q_{22}-Q_{12}-2Q_{66}\right)lm^3\\
\bar{Q}_{26}^{(k)} &= \left(Q_{11}-Q_{12}-2Q_{66}\right)lm^3 - \left(Q_{22}-Q_{12}-2Q_{66}\right)l^3m\\
\bar{Q}_{66}^{(k)} &= \left(Q_{11}+Q_{22}-2Q_{12}-2Q_{66}\right)l^2m^2 + Q_{66}\left(l^4+m^4\right)
\end{aligned} \tag{2}$$

with $l=\cos\theta_k$ and $m=\sin\theta_k$, and are expressed in the x and y directions by considering a fiber orientation angle θ_k (with respect to the x axis) from the constants

$$Q_{11} = \frac{E_L}{1-\nu_{LT}\nu_{TL}}, Q_{22} = \frac{E_T}{1-\nu_{LT}\nu_{TL}},$$
$$Q_{12} = Q_{11}\nu_{TL} = Q_{22}\nu_{LT}, Q_{66} = G_{LT} \tag{3}$$

Here, the subscript L indicates the direction along straight fiber and T does the direction perpendicular to the L axis in the plane. E_L and E_T are young's modulus in the L and T directions, respectively. ν_{LT}, ν_{TL} are the major and minor Poisson's ratios, and G_{LT} is a shear moduli.

In the following numerical examples, a set of constants

$$E_L = 150 \text{ GPa}, E_T = 10 \text{ GPa},$$
$$G_{LT} = 5 \text{ GPa}, \nu_{LT} = 0.3 \tag{4}$$

are used that are the averaged values from a few modern typical CFRP sheets [19].

In the classical lamination theory [1], the in-plane stiffness and bending stiffness are defined by

$$A_{ij} = \sum_{k=1}^{K} \bar{Q}_{ij}^{(k)}\left(z_k - z_{k-1}\right),$$
$$D_{ij} = \frac{1}{3}\sum_{k=1}^{K} \bar{Q}_{ij}^{(k)}\left(z_k^{\,3} - z_{k-1}^{\,3}\right) \tag{5}$$

where K indicates the total number of layers. It is seen that the A_{ij} (i,j=1,2,6) is proportional to z and the D_{ij} (i,j=1,2,6) is to z powered by three.

There is a certain class of laminates that result in $A_{11}=A_{22}$ and $A_{16}=A_{26}=0$, for example in Fig.1, [0/45°/90°/-45°]$_S$ (s denotes symmetric laminate about the mid-plane) with each layer having the same thickness. This specially laminated plate is called "a quasi-isotropic plate", since the plate is uniformly isotropic in the plane (tension). It is noted, however, that the bending stiffness D_{ij} in this case cannot be identical due to "cubic power" of z in Eq.(5) and outer layers contribute more to the bending stiffness of the whole plate.

By generalizing this idea, the following laminated plates are also regarded as quasi-isotropic plates.

Six-layer plate:

$$\left[\theta_1/\theta_2/\theta_3\right]_S, \quad \theta_i \in \left\{\theta_1-60^\circ, \theta_1+60^\circ\right\} \quad (i=2,3) \tag{6}$$

Eight-layer plate:

$$\left[\theta_1/\theta_2/\theta_3/\theta_4\right]_S$$
$$\theta_i \in \left\{\theta_1-45^\circ, \theta_1+45^\circ, \theta_1+90^\circ\right\} \quad (i=2,3,4) \tag{7}$$

Ten-layer plate:

$$\left[\theta_1/\theta_2/\theta_3/\theta_4/\theta_5\right]_S$$
$$\theta_i \in \left\{\theta_1-72^\circ, \theta_1-36^\circ, \theta_1+36^\circ, \theta_1+72^\circ\right\} \quad (i=2,3,4,5) \tag{8}$$

Twelve-layer plate:

$$\left[\theta_1/\theta_2/\theta_3/\theta_4/\theta_5/\theta_6\right]_S$$
$$\theta_i \in \left\{\theta_1-60^\circ, \theta_1-30^\circ, \theta_1+30^\circ, \theta_1+60^\circ, \theta_1+90^\circ\right\}$$
$$\left(i=2,3,4,5,6\right) \tag{9}$$

where θ_1 is any angle (real number) on $-90^\circ < \theta_1 \le 90^\circ$ but for clarity, it is here assumed to be with an increment of $\Delta\theta_1$=5° (i.e., $\theta_1 = -85^\circ,..,0^\circ,5^\circ,10^\circ,..,90^\circ$) or $\Delta\theta_1$=15°.

For example in Eq.(9), θ_1 is a fiber orientation angle of the outer-most layer, θ_2 is an fiber angle of the second outer layer, and θ_6 is an fiber angle of the inner-most layer. So the sequence in bracket [ ] is technically important. In contrast, $\theta_i \in \{\ \}$ simply means that θ_i 's (i=2,3,..) is chosen once among elements in parenthesis { }.

In computation, the fiber angle θ_1 of outer most layer takes discrete values with $\Delta\theta_1$=5° or 15°, and layers in the second and inner layers are taken to satisfy the assumption of in-plane isotropic. For example, when θ_1 of the

outermost layer is taken as θ_1=10°, a six-layer plate chooses θ_2 and θ_3 from {-50°,70°}, and an eight-layer plate does θ_2, θ_3 and θ_4 from {-35°,55°,-80°}. Similarly, a ten-layer plate takes on among {-62°,-26°,46°,82°}, and a twelve-layer plate does among {-50°,-20°,40°,70°,-80°}. All the fiber angles are adjusted to stay within $-90° < \theta \le 90°$, for example, 105° is replaced by -75° (so, the fiber orientation angle is physically identical).

All the fiber angles written in Eqs.(6)-(9) satisfy the stiffness condition (A_{11}=A_{22} and A_{16}=A_{26}=0) as a quasi-isotropic plate, namely, the in-plane stiffnesses in x and y directions are identical, but the bending (out-of-plane) stiffnesses are anisotropic. This is the reason why the laminated quasi-isotropic plates can be a target for stacking sequence optimization in bending frequencies, although "isotropy" may sound far from the stacking sequence optimization.

2.2 Optimization

The frequency parameter for the bending fundamental (lowest) mode is used as an objective function and is maximized or minimized in the present design problem. The design variables are taken to be a set of fiber orientation angles in the K/2 layers of the upper (lower) half of the cross-section. The design problem is stated as

Maximize the frequency parameter Ω_1
subject to the constraints
that A_{11}=A_{22} and A_{16}=A_{26}=0. (10)

or

Minimize the frequency parameter Ω_1
subject to the constraints
that A_{11}=A_{22} and A_{16}=A_{26}=0. (11)

This approach of using each fiber orientation angle directly as a design variable is straightforward, and the number of design variables stays within the applicable range of permutation, namely, all the combinations can be calculated so that direct comparison is possible without using some approximate optimum design methods, such as mathematical programming or heuristic methods, e.g. genetic algorithm (GA) or particle swarm optimization (PSO).

2.3 Outline of vibration analysis

A previous solution is used here as in [20,21] based on the method of Ritz within the classical thin plate theory. This analysis-based solution has a low computational cost and easiness in varying combination in boundary conditions, in contrast to numerical methods such as the finite element method. Figure 2 shows geometry of rectangular plate and the coordinate system, and the dimension of the plate is given by a×b×h (thickness).

The relation between stress and strain is given in Eq.(1). When this equation is integrated over the thickness after multiplying a thickness coordinate z, one gets moment resultant

$$\begin{Bmatrix} M_x \\ M_y \\ M_{xy} \end{Bmatrix} = \begin{bmatrix} D_{11} & D_{12} & D_{16} \\ D_{12} & D_{22} & D_{26} \\ D_{16} & D_{26} & D_{66} \end{bmatrix} \{\kappa\} \tag{12}$$

where the D_{ij} are the bending stiffnesses (5) and $\{\kappa\}$ is a curvature vector given in (15).

When one considers the small amplitude (linear) free vibration of a plate, the deflection w may be written by

$$w(x,y,t) = W(x,y)\sin\omega t \tag{13}$$

where W is the amplitude and ω is a radian frequency of the plate. Then, the maximum strain energy due to the bending is expressed by

$$U_{\max} = \frac{1}{2}\iint_A \{\kappa\}^T \begin{bmatrix} D_{11} & D_{12} & D_{16} \\ D_{12} & D_{22} & D_{26} \\ D_{16} & D_{26} & D_{66} \end{bmatrix} \{\kappa\}\, dA \tag{14}$$

where $\{\kappa\}$ is a curvature vector

$$\{\kappa\} = \left\{ -\frac{\partial^2 W}{\partial x^2} \quad -\frac{\partial^2 W}{\partial y^2} \quad -2\frac{\partial^2 W}{\partial x \partial y} \right\}^T \tag{15}$$

The maximum kinetic energy is given by

$$T_{\max} = \frac{1}{2}\rho h \omega^2 \iint_A W^2 dA \tag{16}$$

where ρ [kg/m^3] is the mass per unit volume.

For the sake of simplicity, non-dimensional quantities are introduced as

$$\xi = \frac{2x}{a}, \eta = \frac{2y}{b} \text{ (non-dimensional coordinates)},$$

$$\alpha = \frac{a}{b} \text{ (aspect ratio)},$$

$$D_0 = \frac{E_T h^3}{12(1-\nu_{LT}\nu_{TL})} \text{ (reference stiffness)} \tag{17}$$

$$\Omega = \omega a^2 \sqrt{\frac{\rho h}{D_0}} \text{ (frequency parameter)}$$

It should be remembered here that regardless of the number of layers, the frequency parameter is normalized with respect to the total thickness h. Namely, a twelve-layer plate has the same total thickness as a six-layer plate in this parameter Ω.

The next step in the Ritz method is to assume that the amplitude as

$$W(\xi,\eta) = \sum_{m=0}^{M-1}\sum_{n=0}^{N-1} A_{mn} X_m(\xi) Y_n(\eta) \tag{18}$$

where A_{mn} are unknown coefficients, and $X_m(\xi)$, $Y_n(\eta)$ are the functions modified later so that any kinematical boundary conditions are satisfied at the edges.

After substituting Eq.(18) into the energies (14) and (16), the stationary value is obtained by

$$\frac{\partial}{\partial A_{\bar{m}\bar{n}}}(T_{\max} - U_{\max}) = 0 \quad (\bar{m} = 0,1,2,..;\bar{n} = 0,1,2,...) \tag{19}$$

Then the eigenvalue equation that contains the frequency parameter Ω is derived as

$$\sum_{m=0}^{M-1}\sum_{n=0}^{N-1}\left[\left(\frac{D_{11}}{D_0}\right)I^{(2200)}+\alpha^2\left(\frac{D_{12}}{D_0}\right)(I^{(2002)}+I^{(0220)})+\alpha^4\left(\frac{D_{22}}{D_0}\right)I^{(0022)}+4\alpha^2\left(\frac{D_{66}}{D_0}\right)I^{(1111)}-\Omega^2 I^{(0000)}\right]_{\bar{m}\bar{m}\bar{n}\bar{n}}\cdot A_{mn}=0$$

$$(\bar{m}=0,1,2,..;\bar{n}=0,1,2,...) \tag{20}$$

where an integral I is the products

$$I^{(\bar{p}\bar{q}\bar{r}\bar{s})}_{mmnn}=\phi^{(\bar{p}\bar{q})}_{mm}\cdot\phi^{(\bar{r}\bar{s})}_{nn} \tag{21}$$

of the two integrals defined by

$$\phi^{(\bar{p}\bar{q})}_{mm}=\int_{-1}^{1}\frac{\partial^{(p)}X_m}{\partial\xi^{(p)}}\frac{\partial^{(q)}X_{\bar{m}}}{\partial\xi^{(q)}}d\xi \tag{22}$$

Equation (20) is a set of linear simultaneous equations in terms of the coefficients A_{mn}, and the eigenvalues Ω may be extracted by using existing eigenvalue subroutines.

The analytical procedure developed this far is a standard routine of the Ritz method, and modification is explained next so as to incorporate arbitrary edge conditions into the amplitude $W(\xi,\eta)$. In the traditional approach, for example, using the beam functions for $X_m(\xi)$ and $Y_n(\eta)$, many different products of regular and hyper trigonometric functions exist for arbitrary conditions and it is difficult to make a unified subroutine to calculate all of the various kinds of integrals.

The present approach introduces a kind of polynomial

$$X_m(\xi)=\xi^m(\xi+1)^{B1}(\xi-1)^{B3}$$
$$Y_n(\eta)=\eta^n(\eta+1)^{B2}(\eta-1)^{B4} \tag{23}$$

where B_1, B_2, B_3 and B_4 are "boundary indices" [20,21] which are added to satisfy the kinematical boundary conditions and are used in such a way as B_i=0 for F (free edge), 1 for S (simply supported edge) and 2 for C (clamped edge). To the C-S-F-F plate, for instance, B_1=2, B_2=1 and B_3=B_4=0 are applied. With the boundary indices B_i's and Eqs.(23), the method of Ritz can accommodate arbitrary sets of the edge conditions, and the integrals (22) can be exactly evaluated.

Table 1. Convergence and comparison of frequency parameters $\Omega=\omega a^2(\rho h/D)^{1/2}$ for quasi-isotropic square plates with eight symmetric layers [0°/45°/90°/-45°]s

	Ω_1	Ω_2	Ω_3	Ω_4	Ω_5
CFFF plate					
6×6	11.091	19.229	51.920	69.812	83.420
8×8	11.088	19.225	51.435	69.784	83.321
10×10	11.087	19.223	51.432	69.780	83.314
FEM [11]	11.095	19.217	51.419	69.803	83.321
dif.(%)	0.07	-0.03	-0.03	0.03	0.01
CSFF plate					
6×6	13.929	39.070	75.022	91.093	114.46
8×8	13.928	39.064	75.008	90.686	113.67
10×10	13.928	39.063	75.006	90.681	113.66
FEM [11]	13.928	39.050	74.990	90.573	113.53
dif.(%)	0	-0.03	-0.02	-0.12	-0.11
SSSS plate					
6×6	46.075	97.548	139.96	175.06	201.26
8×8	46.070	97.537	139.94	174.32	199.04
10×10	46.068	97.533	139.94	174.31	198.99
FEM [11]	46.005	97.292	139.66	173.42	198.28
dif.(%)	-0.14	-0.25	-0.20	-0.51	-0.36
CCCC plate					
6×6	90.050	151.32	212.95	245.80	274.60
8×8	90.050	151.32	212.95	245.62	274.36
10×10	90.050	151.32	212.95	245.61	274.35
FEM [11]	89.817	150.65	212.34	244.00	272.61
dif.(%)	-0.26	-0.44	-0.29	-0.66	-0.63

3. Numerical examples and accuracy of the solution

3.1 Numerical examples

Symmetrically laminated plates with six, eight, ten and twelve layers are given for numerical examples. A six-layer plate has three design variables $\theta_1,\theta_2,\theta_3$, but due to the restriction of quasi-isotropy in Eq.(6), a number of combination of layers is given by 36×2×1=72 for $\Delta\theta_1$ = 5° of six-layer plates. So, seventy-two times of frequency calculation are repeated to find the maximum and minimum ones. Similarly, the numbers of combination of layers are 36×3×2×1=216, 36×4×3×2×1=864 and 36×5×4×3×2×1=4320 for eight-layer, ten-layer and twelve-layer plates, respectively, with $\Delta\theta_1$ = 5°. In other words, a twelve-layer plate needs computation of sixty (=4320/72) times more than a six-layer plate. A short effective computation time of the present Ritz method is fully made use particularly for 12-layer plate. For $\Delta\theta_1$ = 15°, the number of combinations reduces to 24, 72, 288 and 1440 for six-layer, eight-layer, ten-layer and twelve-layer plates, respectively.

The material constants in Eq.(4) are used in the examples. It should be noted again that the frequency parameter Ω is normalized by the total thickness h (i.e. the total thickness of the plates with different number of layers is regarded as the same) in the definition, when one compares effects of fiber orientation angles among plates with different number of layers.

3.2 Convergence and comparison of the solution

Table 1 presents convergence study of the lowest five frequency parameters $\Omega_1 \sim \Omega_5$ with increase of series terms in Eq.(18). Since the amplitude function satisfies kinematical boundary conditions exactly, this Ritz method yields upper-bound solutions, and tends to converge from above. Four sets of boundary conditions are assumed as CFFF (cantilever), CSFF, SSSS and CCCC plates. Each of these four letters correspond in this order to Edge(1), Edge(2), Edge(3) and Edge(4), respectively, in Fig.2. In the table, the lower frequency parameters are converged in values rounded to four significant figures, and even higher frequencies converge well. Based on this test, following results will be obtained by using 10×10 terms.

Table 2. Frequency parameters Ω_1 and lay-up designs of quasi-isotropic square plates (CFFF)($\Delta\theta_1$= 5°).

6-layer plate			8-layer plate		
Order	Ω_1	$[\theta_1/\theta_2/\theta_3]$s	Order	Ω_1	$[\theta_1/\theta_2/\theta_3/\theta_4]$s
1	11.689	[0/ 60/ −60]	1	11.390	[5/ −40/ 50/ −85]
2	(ditto)	[0/ −60/ 60]	2	(ditto)	[−5/ 40/ −50/ 85]
3	11.649	[5/ −55/ 65]	3	11.366	[−10/ 35/ −55/ 80]
4	(ditto)	[−5/ 55/ −65]	4	(ditto)	[10/ −35/ 55/ −80]
5	11.432	[5/ 65/ −55]	5	11.332	[−10/ 35/ 80/ −55]
6	(ditto)	[−5/ −65/ 55]	6	(ditto)	[10/ −35/ −80/ 55]
⋮			⋮		
69	5.098	[70/ −50/ 10]	213	5.335	[−80/ 55/ −35/ 10]
70	(ditto)	[−70/ 50/ −10]	214	(ditto)	[80/ −55/ 35/ −10]
71	5.070	[−65/ 55/ −5]	215	5.326	[−75/ 60/ −30/ 15]
72	(ditto)	[65/ −55/ 5]	216	(ditto)	[75/ −60/ 30/ −15]

10-layer plate			12-layer plate		
Order	Ω_1	$[\theta_1/\theta_2/\theta_3/\theta_4/\theta_5]$s	Order	Ω_1	$[\theta_1/\theta_2/\theta_3/\theta_4/\theta_5/\theta_6]$s
1	11.390	[5/ −31/ 41/ 77/ −67]	1	11.407	[5/−25/ 35/−55/−85/ 65]
2	(ditto)	[−5/ 31/ −41/ −77/ 67]	2	(ditto)	[−5/ 25/−35/ 55/ 85/−65]
3	11.388	[−5/ 31/ −41/ 67/ −77]	3	11.402	[5/−25/ 35/−55/ 65/−85]
4	(ditto)	[5/ −31/ 41/ −67/ 77]	4	(ditto)	[−5/ 25/−35/ 55/−65/ 85]
5	11.375	[−10/ 26/ −46/ 62/ −82]	5	11.389	[−5/ 25/−35/ 85/ 55/−65]
6	(ditto)	[10/ −26/ 46/ −62/ 82]	6	(ditto)	[5/−25/ 35/−85/−55/ 65]
⋮			⋮		
861	5.326	[85/ −59/ 49/ −23/ 13]	4317	5.288	[−80/ 70/−50/ 40/−20/ 10]
862	(ditto)	[−85/ 59/ −49/ 23/ −13]	4318	(ditto)	[80/−70/ 50/−40/ 20/−10]
863	5.297	[80/ −64/ 44/ −28/ 8]	4319	5.288	[85/−65/ 55/−35/ 25/ −5]
864	(ditto)	[−80/ 64/ −44/ 28/ −8]	4320	(ditto)	[−85/ 65/−55/ 35/−25/ 5]

Table 3. Frequency parameters Ω_1 and lay-up designs of quasi-isotropic square plates (CSFF)($\Delta\theta_1$= 5°).

6-layer plate			8-layer plate		
Order	Ω_1	$[\theta_1/\theta_2/\theta_3]$s	Order	Ω_1	$[\theta_1/\theta_2/\theta_3/\theta_4]$s
1	15.769	[20/ −40/ 80]	1	15.420	[25/ −20/ −65/ 70]
2	15.650	[15/ −45/ 75]	2	15.369	[20/ −25/ −70/ 65]
3	15.642	[25/ −35/ 85]	3	15.355	[30/ −60/ −15/ 75]
4	15.279	[30/ −30/ 90]	4	15.280	[30/ −15/ −60/ 75]
5	15.275	[10/ −50/ 70]	5	15.268	[35/ −55/ −10/ 80]
6	14.695	[35/ −25/ −85]	6	15.241	[25/ −65/ −20/ 70]
⋮			⋮		
69	9.155	[85/ −35/ 25]	213	10.121	[80/ −55/ −10/ 35]
70	9.061	[−80/ −20/ 40]	214	9.947	[−85/ −40/ 5/ 50]
71	8.939	[90/ −30/ 30]	215	9.946	[85/ −50/ −5/ 40]
72	8.902	[−85/ −25/ 35]	216	9.881	[90/ −45/ 0/ 45]

10-layer plate			12-layer plate		
Order	Ω_1	$[\theta_1/\theta_2/\theta_3/\theta_4/\theta_5]$s	Order	Ω_1	$[\theta_1/\theta_2/\theta_3/\theta_4/\theta_5/\theta_6]$s
1	15.467	[25/ −47/ −11/ 61/ −83]	1	15.300	[25/−35/ −5/−65/ 55/ 85]
2	15.431	[30/ −42/ −6/ −78/ 66]	2	15.296	[30/ 0/−60/−30/ 60/ 90]
3	15.397	[25/ −47/ −11/ −83/ 61]	3	15.294	[15/−45/ 45/−15/−75/ 75]
4	15.362	[20/ −52/ −16/ 56/ −88]	4	15.279	[20/−40/−10/ 50/−70/ 80]
5	15.361	[30/ −42/ −6/ 66/ −78]	5	15.279	[25/ −5/−35/−65/ 55/ 85]
6	15.296	[25/ −11/ −47/ −83/ 61]	6	15.276	[30/−30/ 0/−60/ 60/ 90]
⋮			⋮		
861	10.176	[85/ −59/ −23/ 13/ 49]	4317	10.246	[−80/−50/−20/ 70/ 10/ 40]
862	10.147	[90/ −18/ −54/ 54/ 18]	4318	10.203	[−85/−55/−25/ 65/ 5/ 35]
863	10.085	[90/ −54/ −18/ 54/ 18]	4319	10.170	[85/−65/−35/ −5/ 55/ 25]
864	10.078	[−85/ −49/ −13/ 59/ 23]	4320	10.168	[90/−60/−30/ 0/ 60/ 30]

Table 4. Frequency parameters Ω_1 and lay-up designs of simply supported quasi-isotropic square plates (SSSS) ($\Delta\theta_1$= 5°).

6-layer plate			8-layer plate		
Order	Ω_1	$[\theta_1/\theta_2/\theta_3]$s	Order	Ω_1	$[\theta_1/\theta_2/\theta_3/\theta_4]$s
1	51.041	[35/ -25/ -85]	1	53.629	[-45/ 45/ 0/ 90]
2	(ditto)	[-35/ 25/ 85]	2	(ditto)	[-45/ 45/ 90/ 0]
3	(ditto)	[-55/ 65/ 5]	3	(ditto)	[45/ -45/ 90/ 0]
4	(ditto)	[55/ -65/ -5]	4	(ditto)	[45/ -45/ 0/ 90]
5	51.006	[-30/ 30/ 90]	5	53.441	[50/ -40/ -85/ 5]
6	(ditto)	[30/ -30/ 90]	6	(ditto)	[-40/ 50/ 5/ -85]
・			・		
69	43.961	[-75/ -15/ 45]	213	44.307	[0/ 90/ -45/ 45]
70	(ditto)	[15/ 75/ -45]	214	(ditto)	[0/ 90/ 45/ -45]
71	(ditto)	[75/ 15/ -45]	215	(ditto)	[90/ 0/ 45/ -45]
72	(ditto)	[-15/ -75/ 45]	216	(ditto)	[90/ 0/ -45/ 45]

10-layer plate			12-layer plate		
Order	Ω_1	$[\theta_1/\theta_2/\theta_3/\theta_4/\theta_5]$s	Order	Ω_1	$[\theta_1/\theta_2/\theta_3/\theta_4/\theta_5/\theta_6]$s
1	53.247	[-50/ 58/ 22/ -14/ -86]	1	53.316	[40/-50/-20/ 70/-80/ 10]
2	(ditto)	[40/ -32/ -68/ 76/ 4]	2	(ditto)	[-50/ 40/ 70/-20/ 10/-80]
3	(ditto)	[-40/ 32/ 68/ -76/ -4]	3	(ditto)	[50/-40/-70/ 20/-10/ 80]
4	(ditto)	[50/ -58/ -22/ 14/ 86]	4	(ditto)	[-40/ 50/ 20/-70/ 80/-10]
5	53.165	[-50/ 58/ 22/ -86/ -14]	5	53.286	[-40/ 50/ 20/-70/-10/ 80]
6	(ditto)	[50/ -58/ -22/ 86/ 14]	6	(ditto)	[-50/ 40/ 70/-20/-80/ 10]
・			・		
861	44.947	[10/ 82/ 46/ -26/ -62]	4317	45.274	[85/ -5/ 25/ 55/-65/-35]
862	(ditto)	[-10/ -82/ -46/ 26/ 62]	4318	(ditto)	[-85/ 5/-25/-55/ 65/ 35]
863	(ditto)	[80/ 8/ 44/ -64/ -28]	4319	(ditto)	[5/-85/ 65/ 35/-25 -55]
864	(ditto)	[-80/ -8/ -44/ 64/ 28]	4320	(ditto)	[-5/ 85/-65/-35/ 25/ 55]

Table 5. Frequency parameters Ω_1 and lay-up design of clamped quasi-isotropic square plates (CCCC)($\Delta\theta_1$= 5°).

6-layer plate			8-layer plate		
Order	Ω1	$[\theta_1/\theta_2/\theta_3]$s	Order	Ω1	$[\theta_1/\theta_2/\theta_3/\theta_4]$s
1	90.923	[85/ -35/ 25]	1	91.320	[-85/ 5/ 50/ -40]
2	(ditto)	[-85/ 35/ -25]	2	(ditto)	[5/ -85/ -40/ 50]
3	(ditto)	[-5/ 55/ -65]	3	(ditto)	[85/ -5/ -50/ 40]
4	(ditto)	[5/ -55/ 65]	4	(ditto)	[-5/ 85/ 40/ -50]
5	90.806	[10/ -50/ 70]	5	91.287	[90/ 0/ -45/ 45]
6	(ditto)	[-10/ 50/ -70]	6	(ditto)	[90/ 0/ 45/ -45]
・			・		
69	86.247	[-40/ 80/ 20]	213	86.3075	[55/ 10/ -80/ -35]
70	(ditto)	[40/ -80/ -20]	214	(ditto)	[-55/ -10/ 80/ 35]
71	(ditto)	[-50/ 10/ 70]	215	(ditto)	[35/ 80/ -10/ -55]
72	(ditto)	[50/ -10/ -70]	216	(ditto)	[-35/ -80/ 10/ 55]

10-layer plate			12-layer plate		
Order	Ω1	$[\theta_1/\theta_2/\theta_3/\theta_4/\theta_5]$s	Order	Ω1	$[\theta_1/\theta_2/\theta_3/\theta_4/\theta_5/\theta_6]$s
1	91.186	[0/ 72/ -72/ -36/ 36]	1	91.216	[85/ -5/-65/ 25/ 55/-35]
2	(ditto)	[90/ -18/ 18/ 54/ -54]	2	(ditto)	[5/-85/-25/ 65/ 35/-55]
3	(ditto)	[0/ -72/ 72/ 36/ -36]	3	(ditto)	[-85/ 5/ 65/-25/-55/ 35]
4	(ditto)	[90/ 18/ -18/ -54/ 54]	4	(ditto)	[-5/ 85/ 25/-65/-35/ 55]
5	91.182	[-85/ -13/ 23/ 59/ -49]	5	91.178	[-85/ 5/ 65/-55/-25/ 35]
6	(ditto)	[5/ 77/ -67/ -31/ 41]	6	(ditto)	[5/-85/-25/ 35/ 65/-55]
・			・		
861	86.252	[55/ 19/ -89/ -17/ -53]	4317	86.198	[50/ 20/ 80/-10/-70/-40]
862	(ditto)	[-55/ -19/ 89/ 17/ 53]	4318	(ditto)	[-50/-20/-80/ 10/ 70/ 40]
863	(ditto)	[35/ 71/ -1/ -73/ -37]	4319	(ditto)	[40/ 70/ 10/-80/-20/-50]
864	(ditto)	[-35/ -71/ 1/ 73/ 37]	4320	(ditto)	[-40/-70/-10/ 80/ 20/ 50]

Accuracy of this method is verified also by comparison with the frequency parameters of quasi-isotropic square plates obtained by the finite element program used in ref.[11]. The square plate is divided by 20×20=400 elements, and good agreement is found with the Ritz method. Differences caused by the FEM (20×20 elements) and present Ritz (10×10 terms) methods are evaluated by

$$\text{Difference}(\%) = (\text{FEM} - \text{Ritz}) / (\text{Ritz}) \times 100 \qquad (24)$$

and included in the table. As seen, the differences are very small and accuracy of the methods is well established.

3.3 Numerical results

Tables 2,3,4 and 5 present top six frequency parameters Ω_1 of the highest (maximum) values and four of the lowest (minimum) values for CFFF (cantilever), CSFF, SSSS and CCCC plates, respectively. Aspect ratio is taken *a/b*=1 (square plate). In each table, results are summarized for symmetrically laminated six-layer, eight-layer, ten-layer and twelve-layer plates. In these tables and hereafter, a symbol of angle '°' is omitted in the tables. Stacking sequence in all these examples is examined to satisfy the quasi-isotropic condition.

In Table 2, a six-layer plate (with minimum number of design variables) gives the highest frequency Ω_1=11.689 among four those of different layer numbers, and a twelve-layer plate has the second highest frequency of Ω_1=11.407. It is interesting to see that eight-layer and ten-layer plates share the identical highest frequency Ω_1=11.390. In other words, restriction of the quasi-isotropic condition imposes laminated plates to have complicated optimizing effect, regardless of general tendency that larger number of design variables generally gives more optimized (higher in this case) values. Similarly, for the minimum frequencies, the lowest frequencies are found in the order of plates with six, twelve, ten and eight layers, not simply following the order of the number of layers.

A CFFF (cantilever) square plate in Table 2 has one symmetry axis (about the boundary conditions) that is perpendicular to the clamped edge (Edge(1) in Fig.2), and frequencies are always obtained as pairs of identical frequency values. However, for a CSFF plate with no symmetry with respect to the boundary condition in Table 3, all the frequencies appear as each being independent value. The maximum values are in the decreasing order of Ω_1=15.769, 15.467, 15.420 and 15.300 of plates with six, ten, eight and twelve layers, respectively.

Next, SSSS plate in Table 4 and CCCC plate in Table 5 are uniformly constrained along the edges, and there are two symmetry axes with respect to boundary condition. So, frequencies are given with a set of four identical values due to the two symmetrical axes. Among the maximum frequencies with different number of layers for SSSS plates in Table 4, the maximum values are in the order of Ω_1=53.629, 53.316, 53.247 and 51.041 of plates with eight, twelve, ten and six layers. Unlike plates with free edges in Tables 2 and 3, a six-layer plate does not give the highest value among the four different layer plates. For a CCCC

Table 6. Frequency parameters Ω1 and lay-up designs of quasi-isotropic 8-layer square plates by using $\Delta\theta_1$= 15°

CFFF plate			CSFF plate		
Order	Ω_1	[θ_1/θ_2/θ_3/θ_4]s	Order	Ω_1	[θ_1/θ_2/θ_3/θ_4]s
1	11.291	[0/ 45/ −45/ 90]	1	15.355	[30/ −60/ −15/ 75]
2	(ditto)	[0/ −45/ 45/ 90]	2	15.280	[30/ −15/ −60/ 75]
3	11.229	[15/ −30/ 60/ −75]	3	15.123	[15/ −30/ −75/ 60]
4	(ditto)	[−15/ 30/ −60/ 75]	4	15.099	[15/ −30/ 60/ −75]
5	11.212	[15/ −30/ −75/ 60]	5	14.755	[30/ −60/ 75/ −15]
6	(ditto)	[−15/ 30/ 75/ −60]	6	14.546	[0/ 45/ −45/ 90]
▪			▪		
69	5.512	[60/ −75/ −30/ 15]	69	10.385	[75/ −60/ −15/ 30]
70	(ditto)	[−60/ 75/ 30/ −15]	70	10.324	[−75/ −30/ 60/ 15]
71	5.326	[75/ −60/ 30/ −15]	71	10.287	[75/ −15/ −60/ 30]
72	(ditto)	[−75/ 60/ −30/ 15]	72	9.881	[90/ −45/ 0/ 45]
SSSS plate			**CCCC plate**		
Order	Ω_1	[θ_1/θ_2/θ_3/θ_4]s	Order	Ω_1	[θ_1/θ_2/θ_3/θ_4]s
1	53.629	[45/ −45/ 90/ 0]	1	91.287	[0/ 90/ −45/ 45]
2	(ditto)	[45/ −45/ 0/ 90]	2	(ditto)	[0/ 90/ 45/ −45]
3	(ditto)	[−45/ 45/ 0/ 90]	3	(ditto)	[90/ 0/ −45/ 45]
4	(ditto)	[−45/ 45/ 90/ 0]	4	(ditto)	[90/ 0/ 45/ −45]
5	51.508	[60/ −30/ −75/ 15]	5	90.915	[15/ −75/ −30/ 60]
6	(ditto)	[−30/ 60/ 15/ −75]	6	(ditto)	[−15/ 75/ 30/ −60]
▪			▪		
69	44.307	[0/ 90/ 45/ −45]	69	86.513	[30/ 75/ −15/ −60]
70	(ditto)	[0/ 90/ −45/ 45]	70	(ditto)	[−30/ −75/ 15/ 60]
71	(ditto)	[90/ 0/ 45/ −45]	71	(ditto)	[60/ 15/ −75/ −30]
72	(ditto)	[90/ 0/ −45/ 45]	72	(ditto)	[−60/ −15/ 75/ 30]

Table 7. Maximum and minimum frequency parameters Ω_1 and their ratios of 8-layered square plates ($\Delta\theta_1$=5°)

Class	BC	$\Omega_{1,max}$	$[\theta_1/\theta_2/\theta_3/\theta_4]_S$	$\Omega_{1,min}$	max/min
1	FFFF	32.632	[45/-45/0/90]	21.951	1.49
2	SFFF	19.842	[45/-45/0/90]	10.818	1.83
	FSFF	(ditto)	[-45/45/90/0]	(ditto)	
	FFSF	(ditto)	[45/-45/0/90]	(ditto)	
	FFFS	(ditto)	[-45/45/90/0]	(ditto)	
3	FSSF	10.567	[45/-45/90/0]	5.402	1.96
	FFSS	(ditto)	[-45/45/90/0]	(ditto)	
	SFFS	(ditto)	[45/-45/90/0]	(ditto)	
	SSFF	(ditto)	[-45/45/90/0]	(ditto)	
4	CFFF	11.390	[5/-40/50/-85]	5.326	2.14
	FFCF	(ditto)	[5/-40/50/-85]	(ditto)	
	FCFF	(ditto)	[85/-50/40/-5]	(ditto)	
	FFFC	(ditto)	[85/-50/40/-5]	(ditto)	
5	FFCS	15.420	[25/-20/-65/70]	9.881	1.56
	FSCF	(ditto)	[-25/20/65/-70]	(ditto)	
	CSFF	(ditto)	[25/-20/-65/70]	(ditto)	
	CFFS	(ditto)	[-25/20/65/-70]	(ditto)	
	FFSC	(ditto)	[65/-70/-25/20]	(ditto)	
	FCSF	(ditto)	[-65/70/25/-20]	(ditto)	
	SCFF	(ditto)	[65/-70/-25/20]	(ditto)	
	SFFC	(ditto)	[-65/70/25/-20]	(ditto)	
6	FFCC	18.381	[45/-45/90/0]	13.299	1.38
	FCCF	(ditto)	[-45/45/0/90]	(ditto)	
	CCFF	(ditto)	[45/-45/90/0]	(ditto)	
	CFFC	(ditto)	[-45/45/0/90]	(ditto)	
7	FSFS	31.645	[-85/50/-40/5]	14.669	2.16
	SFSF	(ditto)	[-5/40/-50/85]	(ditto)	
8	SFSS	35.284	[-10/35/-55/80]	21.303	1.66
	SSSF	(ditto)	[-10/35/-55/80]	(ditto)	
	FSSS	(ditto)	[-80/55/-35/10]	(ditto)	
	SSFS	(ditto)	[-80/55/-35/10]	(ditto)	
9	SFSC	36.404	[10/-35/55/-80]	25.620	1.42
	SCSF	(ditto)	[10/-35/55/-80]	(ditto)	
	FSCS	(ditto)	[80/-55/35/-10]	(ditto)	
	CSFS	(ditto)	[80/-55/35/-10]	(ditto)	
10	SFCF	49.854	[5/-40/50/-85]	23.306	2.14
	CFSF	(ditto)	[-5/40/-50/85]	(ditto)	
	FSFC	(ditto)	[-85/50/-40/5]	(ditto)	
	FCFS	(ditto)	[-85/50/-40/5]	(ditto)	
11	FSSC	52.843	[80/-55/35/-10]	28.227	1.87
	SSFC	(ditto)	[-80/55/-35/10]	(ditto)	
	SFCS	(ditto)	[10/-35/55/-80]	(ditto)	
	SSCF	(ditto)	[-10/35/-55/80]	(ditto)	
	SCFS	(ditto)	[80/-55/35/-10]	(ditto)	
	FCSS	(ditto)	[-80/55/-35/10]	(ditto)	
	CSSF	(ditto)	[10/-35/55/-80]	(ditto)	
	CFSS	(ditto)	[-10/35/-55/80]	(ditto)	
12	SSSS	53.629	[-45/45/0/90]	44.307	1.21
13	FSCC	53.669	[75/-60/30/-15]	31.454	1.71
	FCCS	(ditto)	[-75/60/-30/15]	(ditto)	
	SFCC	(ditto)	[15/-30/60/-75]	(ditto)	
	SCCF	(ditto)	[-15/30/-60/75]	(ditto)	
	CCSF	(ditto)	[15/-30/60/-75]	(ditto)	
	CFSC	(ditto)	[-15/30/-60/75]	(ditto)	
	CCFS	(ditto)	[75/-60/30/-15]	(ditto)	
	CSFC	(ditto)	[-75/60/-30/15]	(ditto)	
14	SSSC	63.588	[80/-55/35/-10]	52.398	1.21
	SCSS	(ditto)	[-80/55/-35/10]	(ditto)	
	CSSS	(ditto)	[10/-35/55/-80]	(ditto)	
	SSCS	(ditto)	[-10/35/-55/80]	(ditto)	
15	SSCC	69.660	[45/-45/90/0]	64.000	1.09
	CCSS	(ditto)	[45/-45/0/90]	(ditto)	
	SCCS	(ditto)	[-45/45/0/90]	(ditto)	
	CSSC	(ditto)	[-45/45/90/0]	(ditto)	
16	FCFC	72.699	[-85/50/-40/5]	34.163	2.13
	CFCF	(ditto)	[-5/40/-50/85]	(ditto)	
17	CFCS	74.720	[5/-40/50/-85]	38.348	1.95
	CSCF	(ditto)	[5/-40/50/-85]	(ditto)	
	FCSC	(ditto)	[-85/50/-40/5]	(ditto)	
	SCFC	(ditto)	[-85/50/-40/5]	(ditto)	
18	CFCC	75.290	[5/-40/50/-85]	41.123	1.83
	CCCF	(ditto)	[5/-40/50/-85]	(ditto)	
	FCCC	(ditto)	[85/-50/40/-5]	(ditto)	
	CCFC	(ditto)	[85/-50/40/-5]	(ditto)	
19	SCSC	83.359	[80/-55/35/-10]	59.843	1.39
	CSCS	(ditto)	[10/-35/55/-80]	(ditto)	
20	CSCC	86.374	[10/-35/55/-80]	72.631	1.19
	CCCS	(ditto)	[10/-35/55/-80]	(ditto)	
	CCSC	(ditto)	[80/-55/35/-10]	(ditto)	
	SCCC	(ditto)	[-80/55/-35/10]	(ditto)	
21	CCCC	91.320	[5/-85/-40/50]	86.308	1.06

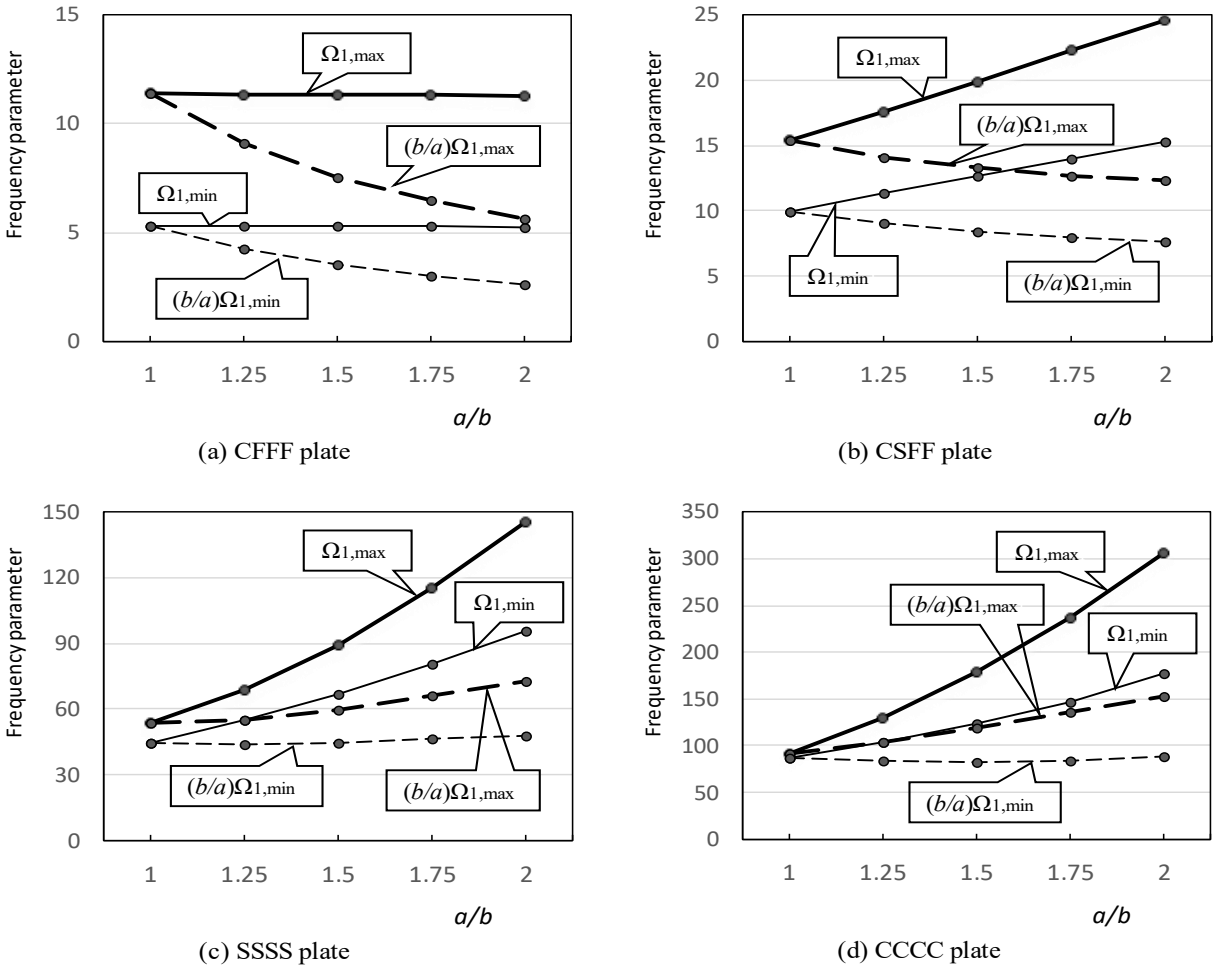

Figure 3. Effect of aspect ratio *a/b* on the maximum and minimum frequencies of quasi-isotropic rectangular plates

plate in Table 5, similarly for a SSSS plate in Table 4, the maximum values are given in the order of eight, twelve, ten and six layers. It is also found that the maximum and minimum frequencies are all close each other due to stronger constraints (i.e., all boundaries clamped) from the edges rather than the constraint from the layer sequence. As mentioned above, the computation time depends on increment $\Delta\theta_1$, and $\Delta\theta_1$=5° was used in Tables 2-5.

Next in Table 6, one sees the effect of using a coarse mesh of $\Delta\theta_1$=15°. This use of the mesh reduces computation time to one third (216 times computation to 72 times) for the eight-layer plate. The table presents top six frequency parameters Ω_1 of the highest values and four of the lowest values for CFFF (cantilever), CSFF, SSSS and CCCC square plates (*a/b*=1). When one compares the maximum frequency $\Omega_{1,max}$, for CFFF plate, it is 11.291/11.390=99.1% of the result with $\Delta\theta_1$=5°. Similarly, reduction of the maximum frequencies is 99.6, 100.0 (same frequency) and 99.5% for CSFF, SSSS and CCCC, respectively. Practically speaking, the results with $\Delta\theta_1$=15° are relatively close to those with $\Delta\theta_1$=5° in these examples.

Table 7 presents $\Omega_{1,max}$, corresponding fiber orientation angles $[\theta_1/\theta_2/\theta_3/\theta_4]_s$ and $\Omega_{1,min}$ with ratios of $\Omega_{1,max}/\Omega_{1,min}$ (ratio of optimization effectiveness) for all possible eighty-one combinations (3^4=81) of *three* classical boundary conditions (F, S, C) along *four* edges of square plates. The eighty-one frequencies are grouped into twenty-one Classes to have identical frequencies. For example, Class 2 (SFFF, FSFF, FFSF, FFFS) holds the same maximum frequency $\Omega_{1,max}$=19.842 and minimum one $\Omega_{1,min}$=10.818.

Class 1 of FFFF plate has three rigid body modes, and Class 2 of SFFF, FSFF, FFSF and SSSF plates has one rigid body mode. These modes in rigid body motion (zero frequency) are not listed here, and the lowest elastic vibration modes are given in the tables. Generally speaking, on the ratio of $\Omega_{1,max}/\Omega_{1,min}$, the ratio decreases from 2.16 of Class 7 (FSFS, SFSF) to 1.06 of Class 21 (CCCC), as the clamped edge (C) is increasing and the free edge (F) is removed along four edges.

For studying effect of aspect ratio *a/b* on the frequencies, Figure 3 presents variations of the maximum frequency $\Omega_{1,max}$ and minimum frequencies $\Omega_{1,min}$ that are shown by *thick* solid line and *thin* solid line, respectively. An aspect ratio *a/b* is covered from *a/b*=1 to 2. Naturally, the thick solid curve in $\Omega_{1,max}$ is always higher than the thin solid curve in $\Omega_{1,min}$, and these curves (thick and thin lines) never cross each other. Since frequency parameter Ω is affected by the change of plate area (i.e., the plate area decreases as *a/b* increases), also shown are broken lines to exclude the effect of plate area. Thick *broken* lines indicate maximum frequency change after excluding the area effect, and the thin *broken* lines do the minimum frequency change by using a modified frequency parameter. This expression can absorb the effect of change in the plate area.

$$\left(\frac{b}{a}\right)\Omega = \omega(ab)\sqrt{\frac{\rho h}{D_0}} \tag{25}$$

In Fig.3 (a) CFFF plate, the maximum $\Omega_{1,max}$ and minimum frequencies $\Omega_{1,min}$ stay almost flat with the aspect ratio change. But after excluding the area effect, both maximum modified parameter $(b/a)\Omega_{1,max}$ and minimum one $(b/a)\Omega_{1,min}$ decrease monotonically. In (b) CSFF plate, $\Omega_{1,max}$ and $\Omega_{1,min}$ linearly increase with a/b. Instead, after removing the area effect, both curves of $(b/a)\Omega_{1,max}$ and $(b/a)\Omega_{1,min}$ become almost linearly go down. As the plate edges are more restrained in (c) SSSS and (d) CCCC plates, $\Omega_{1,max}$ and $\Omega_{1,min}$ increase like a part of quadratic curve. After removal of the area effect, $(b/a)\Omega_{1,max}$ and $(b/a)\Omega_{1,min}$ slightly increase.

4. Conclusions

A quasi-isotropic plate is defined as a laminated composite plate consisting of layers with different fiber orientation angles arranged such that the resulting in-plane stiffness is isotropic. This configuration is achievable because the extensional stiffness matrix is obtained as the linear summation of the stiffness contributions of individual layers. In contrast, the bending stiffness components of a quasi-isotropic laminate are generally not isotropic, since they are proportional to the cubic power of the thickness coordinate, which introduces directional dependence in bending behavior. The present paper noticed this effect and used for optimization.

Quasi-isotropic laminate is widely used in aeronautical structures and related fields. Structural panels in aircraft and spacecraft frequently often employ quasi-isotropic laminates, because they must endure severe multi-directional dynamic conditions during take-off and launch. It is hoped that the idea of present paper will be used in such design situations.

References

[1] Jones RM, Mechanics of Composite Materials, CRC Press, (1998).

[2] Vinson JR, Sierakowski RL, The Behavior of Structures Composed of Composite Materials, Kluwer Academic Pub., (2002).

[3] Phiri R, Rangappa SM, Siengchin S, Oladijo OP, Ozbakkaloglu T, Advances in lightweight composite structures and manufacturing technologies: A comprehensive review, Heliyon, 10 (2024).

[4] Gurdal Z, Haftka RT, Hajela P, 1999, Design and Optimization of Laminated Composite Materials, Wiley-Interscience.

[5] Ghiasi H, Pasini D, Lessard DL, Optimum stacking sequence design of composite materials Part I: Constant stiffness design, Composite Structures 90 (2009), pp.1–11.

[6] Ghiasi H, Fayazbakhsh K, Lessard DL, Optimum stacking sequence design of composite materials Part II: Variable stiffness design, Composite Structures, 93 (2010), pp.1-13.

[7] Bert CW, Optimal design of a composite-material plate to maximize its fundamental frequency, Journal of Sound and Vibration, 50 (1977), pp.229-237.

[8] Fukunaga H, Sekine H, Sato M, Optimal design of symmetrically laminated plates for the fundamental frequency, J. Sound and Vibration, 171, (1994), pp.219-229.

[9] Narita Y, Layerwise optimization for the maximum fundamental frequency of laminated composite plates, Journal of Sound and Vibration, 263, (2003), pp.1005-1016.

[10] Narita Y, Hodgkinson JM, Layerwise optimization for maximising the fundamental frequencies of point-supported rectangular laminated composite plates, Composite Structures, 69 (2005), pp.127-135.

[11] Narita Y, Maximum frequency design of laminated plates with mixed boundary conditions, International Journal of Solids and Structures, 43, (2006), pp.4342-4356.

[12] Honda S, Narita Y, Sasaki K, Discrete optimization for vibration design of composite plates by using lamination parameters, Advanced Composite Materials 18 (2009), pp.297-314.

[13] Fukunaga H, On isotropic laminate configurations, Journal of Composite Materials, 24, (1990), pp.519-535.

[14] Paradies R, Designing quasi-isotropic laminates with respect to bending, Composites Science and Technology, 56, (1996), pp.461-472.

[15] Akkerman R, On the properties of quasi-isotropic laminates, Composites Part B, 33, (2002), pp.133-140.

[16] Douglas L, Otterloo V, Dayal V, How isotropic are quasi-isotropic laminates, Composites Part.A, 34 (2003), pp.93-103.

[17] Vannucci P, Verchery G, A new method for generating fully isotropic laminates, Composite Structures, 58 (2002), pp.75-82.

[18] Altunsaray E, Bayer I, Deflection and free vibration of symmetrically laminated quasi-isotropic thin rectangular plates for different boundary conditions, Ocean Engineering, 57 (2013), pp.197-222.

[19] Narita Y, Innami M, Narita D, The effect of using different elastic moduli on vibration of laminated CFRP rectangular plates, EPI Int. J. Engng, 2 (2019). pp.19-27. DOI: 10.25042/epi-ije.022019.05

[20] Narita Y, Combinations for the free-vibration behaviors of anisotropic rectangular plates under general edge conditions, Trans. ASME, J. Appl. Mech., 67 (2000), pp.568-573.

[21] Narita Y, Natural frequencies of isotropic rectangular plates in improved accuracy, EPI Int. J. Eng, 5 (2022), pp. 26-36. DOI: 10.25042/epi-ije.022022.05.